Control design issues for a microinvasive neurosurgery teleoperator system

Jacopo Semmoloni, Rudy Manganelli, Alessandro Formaglio and Domenico Prattichizzo

***Abstract*— This paper deals with controller design issues for a neurosurgical teleoperator system. The specific application of interest consists in remotely inserting a linear-stage rigid endoscope into the patient's brain for microinvasive neurosurgery interventions. This work aims at evaluating the applicability of an existing general-purpose control architecture, addressing its advantages and drawbacks with respect to a simple task-oriented architecture, specifically designed for the target application. Preliminary experiments revealed that the task-oriented design can better fit the application requirements.**

I. INTRODUCTION

In the last years, the usage of robotic teleoperation systems in the operation room is increasing fast [1]. Among the large variety of applications dealing with this research, in this paper the attention is directed towards microinvasive neurosurgery. This work is part of the project *RoboCAST: ROBOt and sensors integration for Computer Assisted Surgery and Therapy* [2]. According to the project goals, the telemanipulation system is targeted at driving the insertion of a linear-stage rigid endoscope into the brain of the patient for neurosurgery interventions. The endoscope insertion will be assisted by a haptic interface, which will extend and complement the surgeons skills during the insertion process. The device will be responsible for the reproduction and the eventual amplification of the forces experienced by the end-effector linear stage via a force feedback interface onto the surgeons hand. This mechanism will enable the manual servo-assisted insertion of the probe into soft tissues without the loss of kinaesthetic perception.

In this paper we present preliminary results of our current research, addressed towards the design issues characterizing teleoperation control systems. The goal of a teleoperation controller is to achieve transparency while maintaining stability (i.e., such that the system does not exhibit vibration or divergent behavior), under any operating conditions and for any environments [3], [4], [5], [6]. To this end, the control architectures are designed trading off transparency and stability, since transparency must often be sacrificed in order to guarantee stable operation in the wide range of environment impedances [7], [8].

We remark that we are far from providing a fair comparison between different control architectures available in the literature. The target of this preliminary work was evaluating the possibility to adapt existing control schemes to the application of interest, before undertaking the development of a new specific and task-oriented architecture. After a brief review of the literature, we chose to evaluate the applicability of the Time-Domain Passivity Control (PC) introduced in [9]. Then, we developed a simple task-oriented proportional-derivative (PD) control based on the assumption that the user's commanded motions during a microinvasive neurosurgery intervention will be slow and sharp, thus also the force reflection will be fed back with slow dynamics. Hence, the PD has been designed in order to filter out all surgeons motions exceeding a predefined bandwidth, thus privileging task accuracy and safety in spite of a loss of dynamical performance.

The testbed setup was a master-slave system composed by a Omega Haptic Device (master) and a KUKA KR3 robot (slave). We qualitatively evaluated the system performance in three telemanipulation tasks: rigid contact with high stiffness objects, soft contact with a deformable object and finally the insertion of a needle into a perforable material. The results stemming from this preliminary study show that in spite of its simplicity, the task-oriented design fits better the requirements for the application of interest.

The remainder of this paper is structured as follows: in Section II we model the teleoperation system, the Section III discusses the adopted control strategies, the Section IV reports experiments and results, and finally the Section V concludes this work.

II. MODELING

The teleoperator system is modeled as the combination of three subsystems: the master device, the slave device and the controller, as shown in Fig. 1. In the scope of this work, each subsystem is modeled as a linear time-invariant (LTI) system.

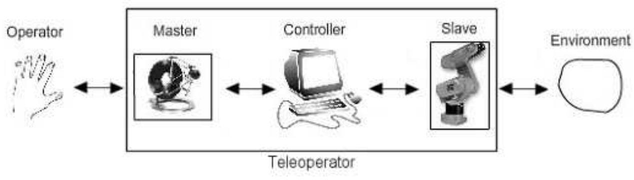

Fig. 1. The functional scheme of a teleoperator system.

The master system is the device that the user remotely handles to drive the endoscope insertion, while the slave

This work was supported by the European Community under Grant FP7-ICT-2007-215190 RoboCAST.

Jacopo Semmoloni, Rudy Manganelli, Alessandro Formaglio and Domenico Prattichizzo are with Department of Information Engineering, University of Siena, via Roma 56, 53100 Siena, Italy. semmoloni@gmail.com, manganelli@dii.unisi.it, formaglio@dii.unisi.it, prattichizzo@dii.unisi.it

physically performs the task in the operational environment. In this application, the master is the Omega.3 impedance force-feedback device (ForceDimension), whose technical specifications are reported in Table I.

Kinematics	Parallel - 3 DoF
Workspace	$160 \times 160 \times 120mm$
3D Resolution	$< 0.01mm$
Stiffness	$15N/mm$
Peak Force	$12N$
Max Continuous Force	$12N$

TABLE I
TECHNICAL SPECIFICATIONS OF THE OMEGA.3 HAPTIC INTERFACE.

As already mentioned in the introduction, the final application consists in driving the insertion of a linear-stage endoscope, hence the task will feature a single translational DoF. To that end, we chose to mechanically customize the kinematics of the Omega in order to constrain the possible motion only along a single DoF, as shown in Fig. 2.

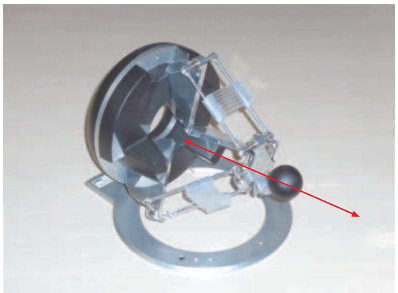

Fig. 2. The customized Omega.3 featuring a single translational DoF.

The slave device is the anthropomorphic manipulator KUKA KR3. The Table II reports the main technical specifications of the slave robot. The KR3 is a discrete-time system

Kinematics	anthropomorphic - 6 DoF
Workspace	Max reach 650mm
3D Resolution	$0.001mm$
Repeatability	$< \pm 0,02mm$
Peak Force	$35N$
Max Velocity	$5m/sec$

TABLE II
TECHNICAL SPECIFICATIONS OF THE KR3 MANIPULATOR.

featuring sampling time $T_s = 12ms$, its end-effector motion can be controlled by applying force or velocity reference signals, defined in the joint space or in the operational space. In the application of interest, we chose the operational space velocity control. Hence, for the sake of simplicity, we modeled the slave dynamics as an integrator with one-step time delay, yielding the transfer function $H(z)$:

$$H(z) = \frac{T_s}{z(z-1)} \tag{1}$$

In order to measure the forces due to the interaction with the operational environment, the slave end-effector was equipped with a 1-DoF force sensor, featuring 4 wheatstone-bridge strain gauges. The data acquisition setup, including the sensor power supply and a National Instrument 6014-PCI acquisition device, was tuned to measure forces ranging from $-12N$ to $12N$, with a resolution of $0.4mN$.

III. TELEMANIPULATION CONTROL

As already mentioned in the introduction, we implemented the time-domain passivity control. Using this approach, the teleoperation system can be modeled as a two-port network as the one depicted in Fig. 3. where the human operator's

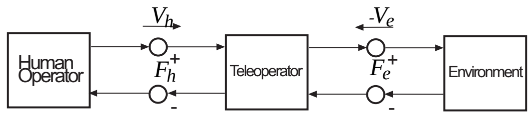

Fig. 3. The master-slave teleoperation system, modeled as a two-port network

force F_h and the remote environment force F_e are the efforts, and the master end-effector velocity V_h and the slave end-effectors velocity V_e are the flows. The stability of the overall system is then ensured provided that each port is passive, i.e. it does not introduce energy into the system [9].

A passivity observer (PO) is applied to monitor the port energy at each time instant. Assuming that the controller is a discrete-time system featuring sample time T_c, the PO computes the port energy at the k^{th} time instant as:

$$E_{PO}(k) = E_{PO}(k-1) + T_c F(k) V(k)$$

Hence the network port is passive until $E_k \geq 0$, otherwise the port is generating energy, and the system stability is no more guaranteed. In addition to detecting a violation of passivity condition, the PO is able also to quantify the amount of energy that is being introduced into the system. This information is used to set up a passivity controller α to dissipate such an amount of energy, in order to restore the port passivity. The passivity controller (PC) is defined by the following control equations:

$$\begin{aligned} & F_h(n) = F_e(n) \\ & \frac{1}{\alpha(n)} = \begin{cases} -\frac{E_{PO}(n)}{\Delta T F_e(n)^2} & if E_{PO} < 0 \\ 0 & if E_{PO} \geq 0 \end{cases} \\ & V_h(n) = V_e(n) + \frac{1}{\alpha(n)} F_e(n) \end{aligned} \tag{2}$$

The teleoperator system with the passivity controller is then represented by the block scheme depicted in Fig. 4.

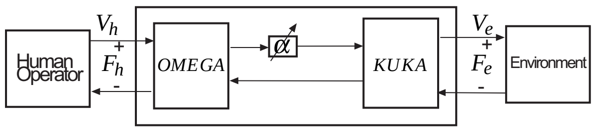

Fig. 4. The master-slave teleoperator system with the passivity controller α.

In order to filter out the noise from the velocity signals the discrete-time First Order Adaptive Windowing (FOAW) filter introduced in [10] has been implemented. It originates from common FIR filters but uses adaptive windowing. Hence, it minimizes the velocity error variance while maximizes the accuracy of the estimates, requiring no tradeoff between noise reduction, control delay, estimate accuracy, reliability, computational load, transient preservation, and difficulties with tuning. The time window size is set as the maximum size such that the straight line joining the extreme samples passes through the uncertainty interval of each sample falling inside the window. Hence, as the size n is adapted, the velocity sample $\hat{V}(k)$ at time instant k is computed as:

$$\hat{V}(k) = \frac{1}{nT_c}(X(k) - X(k-n)) \tag{3}$$

where $X(k)$ is the end-effector position at time instant k.

The main advantage of this general-purpose approach consists of its independency from the dynamical models of the master and of the slave devices, which makes it usable with any hardware setup. On the other hand, the main drawback of this technique is that the control effort determined by the PC can lead to actuator saturation. Generally, in order to prevent saturation, the PC signal is upper bounded, but this in turn can reflect in a drop of performance. In fact, in such a case the dissipation of the exceeding energy may require more than one time step, leading to transient vibration effects.

A simpler control strategy has been designed for this teleoperation system relying on the assumption that the user's commanded motions during microinvasive neurosurgery interventions will be slow and sharp, thus also the force reflection will be fed back with slow dynamics. Hence, we designed a simple proportional-derivative (PD) controller in order for the slave end-effector to track the master end-effector motion, filtering out all frequency contents exceeding a predefined bandwidth. Hence, the PD transfer function $C(z)$ is defined as:

$$C(z) = k_P - \frac{z-1}{T_s z} k_D \tag{4}$$

The block scheme for the teleoperation system can be simply represented as:

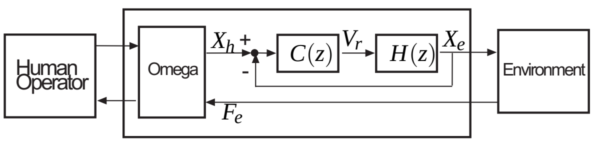

Fig. 5. The master-slave teleoperator system with the PD controller.

where X_h and X_e are the master and slave end-effector positions respectively, V_r is the velocity reference for the slave and F_e is the force measured by the slave sensor. Again, the FOAW filter was adopted in order to filter out the noise from the velocity signals.

IV. EXPERIMENTS

Several experiments have been carried out to evaluate the performance of the teleoperation system using the passivity control (PC) and the low-pass proportional-derivative (PD) control. In this experimental campaign, our design specifications for the PD controller were oriented to filter out all movements exceeding a bandwidth of $2Hz$, yielding $k_P = 3$ and $k_D = 0.35$. We remark that this choice was adopted taking into account that this work is addressed to a microinvasive neurosurgery application, hence the accuracy and safety during task completion are privileged in spite of a loss of dynamical performance.

In the following, we report the results achieved in three teleoperation tasks: rigid contact, soft contact and needle insertion. For each task, we recorded position, velocity and force of both master and slave end-effectors.

Fig. 6. First task: rigid contact with a high stiffness object.

In the first task, the contact with a rigid wall was performed, as shown in Fig. 6. The experimental data acquired using the PC control and the PD control are shown in Fig. 7 and Fig. 8 respectively.

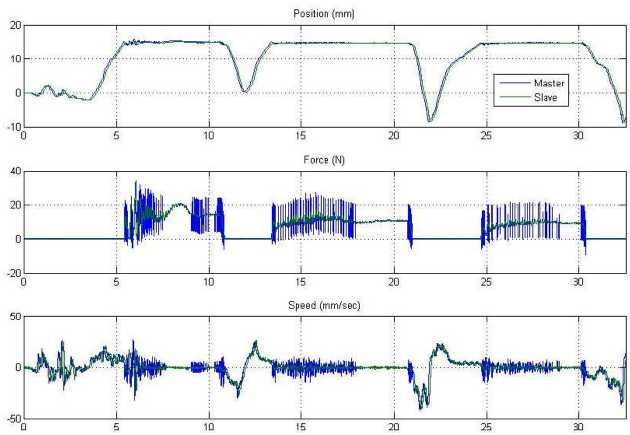

Fig. 7. Trajectories and energies for a rigid contact using PC control.

The second task consisted in remotely touching the foam rubber dice depicted in Fig. 9, whose stiffness has been estimated about $100\frac{N}{m}$. The Fig. 10 and Fig. 11 show the data recorded during the contact, using the PC control and the PD control.

Finally, the third task consisted in remotely inserting a syringe needle into an organic material. To this end, the needle was rigidly attached to the slave end-effector, as

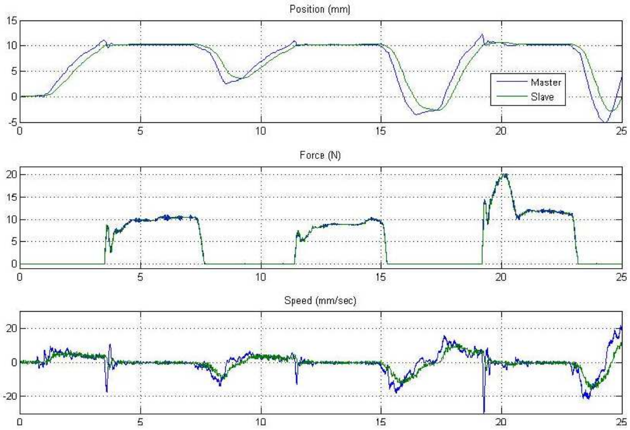

Fig. 8. Trajectories and energies for a rigid contact using PD control.

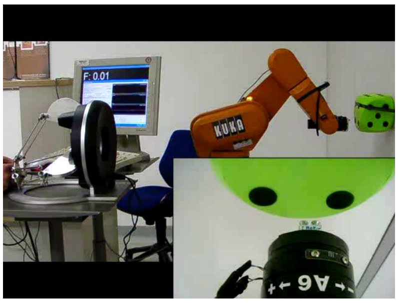

Fig. 9. Second task: soft contact with a deformable object.

shown in Fig. 12. We were interested in experiencing the effects of penetration and of viscous dumping due to the perforation of the skin and of the internal pulp. In this experiment, as target object we chose a kiwi. As it was expected, the forces stemming from this type of interaction were almost impossible to be perceived by the user, hence it was required to amplify the measured forces. The Fig. 13 and Fig. 14 show the trajectories recorded during the contact, using the PC control and the PD control, and amplifying the forces with a gain $k = 10$.

The PC was able to restore the system passivity every time it was required during all tasks, thus guaranteeing the stability. Using the PD controller, the system was always stable. In terms of master-slave position tracking, in the rigid contact the PC performance were slightly higher than for the PD, while in the other tasks there are no significant differences. On the other hand, as regards the haptic feedback, the PD was always able to render smooth contact forces, while the PC generally delivered noisy force profiles. This can be ascribed to the PC efforts required to restore the system passivity. Recall that as soon as the passivity observer reveals that the energy is negative, the controller attempts to dissipate such an amount of energy, possibly in a single step. Hence the PC impulsive control efforts can affect the haptic feedback, providing a noisy force profile.

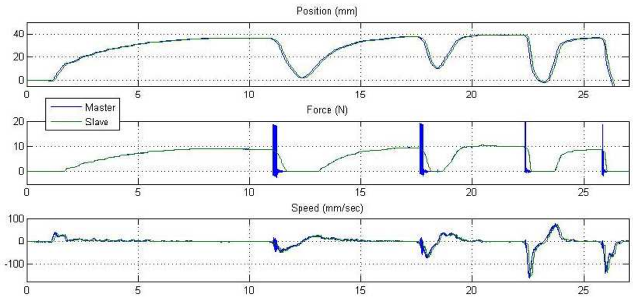

Fig. 10. Trajectories and energies for a soft contact using PC control.

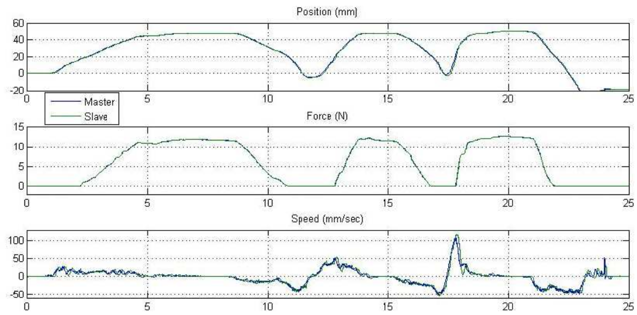

Fig. 11. Trajectories and energies for a soft contact using PD control.

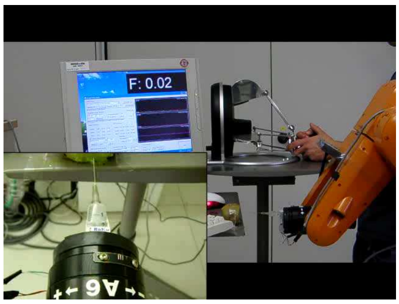

Fig. 12. Third task: insertion of a needle into a perforable material.

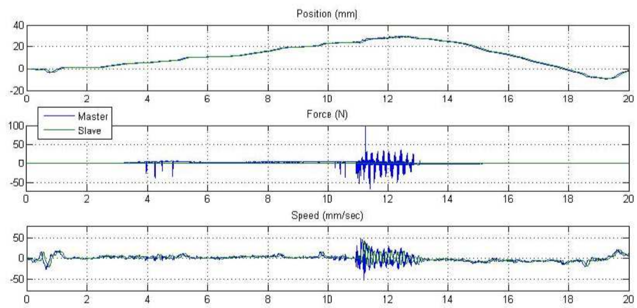

Fig. 13. Trajectories and energies for needle insertion using PC control.

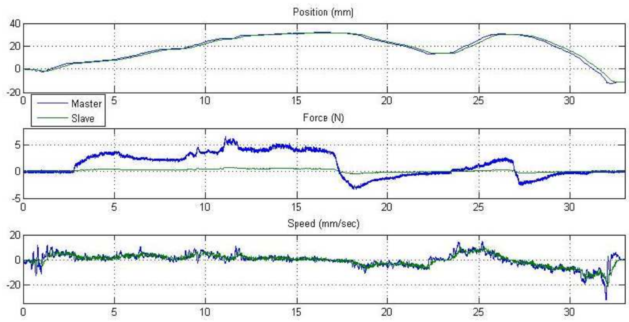

Fig. 14. Trajectories and energies for needle insertion using PD control.

V. DISCUSSION AND CONCLUSION

This paper addresses design issues characterizing a teleoperation control system targeted at driving the insertion of a linear-stage rigid endoscope into the brain of the patient for neurosurgery interventions. This activity is part of the project *RoboCAST: ROBOt and sensors integration for Computer Assisted Surgery and Therapy*. We present preliminary results of our current research, addressed towards evaluating the applicability of a general-purpose control scheme compared to a specific and task-oriented architecture.

The general-purpose control scheme we chose is the Time-Domain Passivity Control. Then, the task-oriented scheme is a proportional-derivative control, based on the assumption that during microsurgery interventions the user's commanded motions and the reflected forces will be characterized by slow dynamics. Hence, the PD was designed in order to filter out all surgeons motions exceeding a predefined bandwidth, thus privileging task accuracy and safety in spite of a loss of dynamical performance.

The experimental setup was a master-slave system composed by a Omega Haptic Device (master) and a KUKA KR3 robot (slave).

Three tasks were experimented to qualitatively evaluate the system performance: rigid contact with high stiffness objects, soft contact with a deformable object and finally the insertion of a needle into a perforable material. The results stemming from this preliminary study show that even if the task-oriented design provides lower dynamical performance than the general-purpose one, it revealed to be stable and was able to render smoother forces in any situation, improving the user's kinesthetic perception during the the task remote control.

Among the future perspectives in this research, we planned a further development of the task-oriented design, in order to improve dynamical performance and to formalize the stability analysis.

VI. ACKNOWLEDGMENTS

This work has been supported by the European Community under Grant FP7-ICT-2007-215190 RoboCAST. We wish to thank also Francesco Chinello for his precious collaboration.

REFERENCES

[1] P. Hokayem and M. Spong, "Bilateral teleoperation: An historical survey," *Automatica*, vol. 42, no. 12, pp. 2035–2057, 2006.

[2] "RoboCAST: ROBOt and sensors integration for Computer Assisted Surgery and Therapy - Grant FP7-ICT-2007-215190 - http://www.robocast.eu/."

[3] B. Hannaford, "A design framework for teleoperators with kinesthetic feedback," *IEEE transactions on Robotics and Automation*, vol. 5, no. 4, pp. 426–434, 1989.

[4] J. Ryu and D. Kwon, "A novel adaptive bilateral control scheme using similar closed-loop dynamic characteristics of master/slave manipulators," *Journal of Robotic Systems*, vol. 18, no. 9, pp. 533–543, 2001.

[5] R. Anderson and M. Spong, "Asymptotic stability for force reflecting teleoperators with time delay," *The International Journal of Robotics Research*, vol. 11, no. 2, p. 135, 1992.

[6] S. Salcudean, "Control for teleoperation and haptic interfaces," *Lecture Notes in Control and Information Sciences*, pp. 51–66, 1998.

[7] R. Adams and B. Hannaford, "Stable haptic interaction with virtual environments," *IEEE Transactions on robotics and Automation*, vol. 15, no. 3, pp. 465–474, 1999.

[8] J. Colgate, "Robust impedance shaping telemanipulation," *IEEE transactions on Robotics and Automation*, vol. 9, no. 4, pp. 374–384, 1993.

[9] J. Ryu, D. Kwon, and B. Hannaford, "Stable teleoperation with time-domain passivity control," *IEEE Transactions on robotics and automation*, vol. 20, no. 2, pp. 365–373, 2004.

[10] F. Janabi-Sharifi, V. Hayward, and C. Chen, "Discrete-time adaptive windowing for velocity estimation," *Control Systems Technology, IEEE Transactions on*, vol. 8, no. 6, pp. 1003–1009, 2000.